analytical chemistry

Article

pubs.acs.org/ac

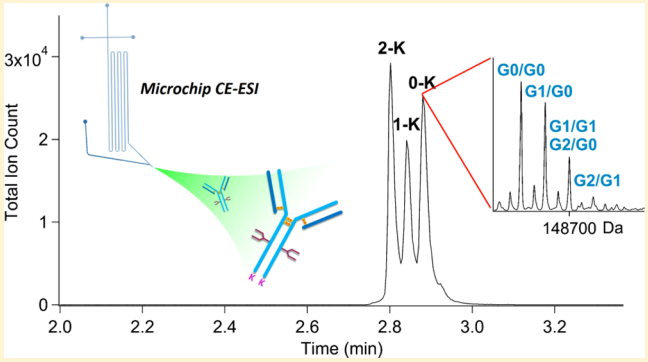
Integrated Microfluidic Capillary Electrophoresis-Electrospray Ionization Devices with Online MS Detection for the Separation and Characterization of Intact Monoclonal Antibody Variants

Erin A. Redman,[†] Nicholas G. Batz,[†] J. Scott Mellors,[†] and J. Michael Ramsey*[,†,‡,§,∥]

[†]Department of Chemistry, [‡]Department of Applied Physical Sciences, [§]Department of Biomedical Engineering, [∥]Carolina Center for Genome Sciences, University of North Carolina, Chapel Hill, North Carolina 27599, United States

Supporting Information

ABSTRACT: Here, we demonstrate an integrated microfluidic capillary electrophoresis-electrospray ionization (CE-ESI) device for the separation of intact monoclonal antibody charge variants with online mass spectrometric (MS) identification. The need for dynamic coating and zwitterionic background electrolyte (BGE) additives has been eliminated by utilizing surface chemistry within the device channels to control analyte adsorption and electroosmotic flow (EOF) while maintaining separation efficiency. The effectiveness of this strategy was illustrated with the separation of charge variants of Infliximab. Three major species corresponding to C-terminal lysine variants were separated with an average resolution of 0.80 and identified by mass difference. In addition to the lysine variants, masses were determined for minor acidic and basic species. The separation of these variants prior to MS analysis facilitated the identification of glycosylation patterns for each of the variants. The general applicability of this method was demonstrated by analyzing two additional monoclonal antibody species: an IgG2 antibody and an IgG1 antibody conjugate. The IgG2 proved to have similar modifications to Infliximab with lower relative abundances of the lysine variants. Analysis of the IgG1 drug conjugate further exemplified the advantages of MS detection; differences in the extent of antibody conjugation were detectable despite limited CE resolution. The CE-ESI-MS methodology described here is a rapid and generic strategy for the separation of intact mAb charge variants and facilitates the identification of variants through MS detection.



Biotherapeutics, monoclonal antibodies (mAbs) in particular, represent a multibillion dollar industry that continues to expand. In order to be used as a therapeutic agent, the biomolecule must be rigorously characterized in order to ensure safety, efficacy, and potency. However, the size and complexity of mAbs makes this a challenging task. Most therapeutic mAbs are γ-immunoglobulins (IgGs) with molecular weights of approximately 150 kDa.[1−5] Throughout cell culture production, purification, and storage, variations in the mAb structure can result from modifications at the primary and secondary structure level.[5,6] Such modifications may include disulfide bond scrambling, glycosylation, deamidation, pyroglutamate formation, C-terminal lysine truncation, oxidation, and amino acid substitutions/misincorporations, in addition to others, and can potentially impact the immunogenic properties of the mAb. Individually, these modifications can introduce a significant amount of heterogeneity in the final product, and it is likely that mixtures of multiple modifications will coexist in finished products that may ultimately increase upon storage or degradation.[1,4,7,8] Consequently, it is critical to characterize such molecules from the amino acid sequence to structural conformation to ensure clinically significant bioactivity, drug effectiveness, and quality. Common techniques used to analyze mAbs include chromatographic methods such as size exclusion chromatography, ion-exchange chromatography, reversed-phase liquid chromatography, and electrophoresis based methods such as isoelectric focusing, gel electrophoresis, and capillary zone electrophoresis. Each technique contributes complementary information to the overall characterization of the mAb, but currently, there is no single technique capable of generating all of the desired information about mAb heterogeneity.

Electrospray ionization mass spectrometry is a powerful technique for mAb characterization due to the ability to assign mass values to many structural variants. An average molecular weight (MW) as well as significant mass shifts (such as those arising from glycosylation) can often be determined by direct infusion into a mass spectrometer. However, as the heterogeneity of the mAb population increases so does the complexity of the mass spectrum, and the isotopic distribution of an intact mAb (~25 Da at half height) combined with additional mass spectral peak broadening obscures minor mass variations such as those due to deamidation and oxidation

Received: October 23, 2014
Accepted: January 8, 2015
Published: January 8, 2015

© 2015 American Chemical Society

DOI: 10.1021/ac503964j
Anal. Chem. 2015, 87, 2264−2272

unless unit mass resolution can be achieved.[2−4,6,9] It has been shown that a resolving power in excess of 400 000 is required to achieve unit mass baseline resolution of molecules of the size and complexity of mAbs.[10] A more accessible solution to the problem of spectral overlap is to include a separation step prior to mass spectrometric (MS) analysis.

Many mAb modifications induce a change in net charge, and therefore, mAb variants can be separated on the basis of charge differences. However, the most common analysis techniques for assessing mAb charge heterogeneity, such as ion-exchange chromatography (IEX) and isoelectric focusing, do not directly interface well with MS. To separate charge variants, these techniques typically require mobile phases or background electrolytes that are not compatible with electrospray ionization (ESI).[2,9,11−13] Thus, they are almost exclusively relegated to optical detection methods, requiring additional analysis to identify the observed peaks. Efforts have been made to develop MS compatible methodology for these techniques, but they have yet to result in the successful separation of intact mAb charge variants with identification by online MS analysis.[14−16]

Capillary electrophoresis (CE) is another method that can be used to separate intact mAb variants that is potentially compatible with MS detection. The CE separation mechanism is based on differences in electrophoretic mobility, which is determined by the charge and size of analyte molecules. All successful CE methods must control analyte adsorption, maintain solubility, and enhance mobility differences between species, all of which tend to become more challenging as the size and complexity of the analyte increases.[2,17−20] While CE-MS has been successfully demonstrated for the analysis of enzymatically digested mAbs and substantially smaller intact proteins,[21−28] previous work using CE for intact mAb analysis has been limited to optical detection and MS compatibility was not a consideration during method development. Consequently, separation background electrolytes (BGEs) have included mixtures of components that facilitate the separation but preclude the use of ESI. For instance, triethylenetetramine (TETA) and high levels of ε-amino-caproic acid (EACA) are often added to the BGE. TETA acts as a dynamic coating to prevent analyte adsorption, and EACA is a zwitterion that can be used to create high ionic strength, low conductivity buffers that reduce electroosmotic flow (EOF) and enhance electrophoretic mobility differences.[29−33] This strategy results in the separation of charge variants, but the complexity and nature of the BGE components render it incompatible with ESI-MS. Thus, the same problems encountered with ion-exchange chromatography and isoelectric focusing exist.

Our strategy for performing CE-ESI-MS has been to use microfluidic technology to eliminate sources of extra-column band broadening and surface coatings to control analyte adsorption; this has resulted in highly efficient separations of biomolecules using ESI compatible BGEs.[34−38] For mAb analysis, a surface coating method utilizing chemical vapor deposition (CVD) of an aminopropylsilane (APS) base layer[38] and covalent modification with polyethylene glycol (PEG) is used to prevent analyte adsorption and reduce the EOF. The uniformity and stability of this surface coating yields highly efficient separations. Additionally, the EOF reduction enhances differences in the electrophoretic mobility of the charge variants and increases the resolution of the separation without the use of surfactants or high ionic strength buffers. This eliminates the need for additives such as TETA and EACA so a simple MS compatible BGE can be used without sacrificing separation performance. The APS-PEG surface coating strategy in conjunction with the zero dead volume integration of microfluidic CE-ESI devices results in the successful separation of intact mAb charge variants with online MS analysis. The device performance is demonstrated by characterizing C-terminal lysine variants of a commercial biotherapeutic IgG as well as two additional mAbs.

EXPERIMENTAL SECTION

Materials and Reagents. Deionized water was generated with a Nanopure Diamond water purifier (Barnstead International, Dubuque, IA). Optima LC/MS grade 2-propanol and acetic acid (99% purity) were obtained from Fisher Scientific (Fairlawn, NJ). The silane coating reagent 3-(aminopropyl)diisopropyl-ethoxysilane (APDIPES) was purchased from Gelest (Morrisville, PA) and the methyl-terminated polyethylene glycol *n*-hydroxy succinimide ester (NHS-PEG$_{450}$) was purchased from Nanocs Inc. (Boston, MA). The number designation 450 denotes the number of PEG units in the reagent. Trichloro(1*H*,1*H*,2*H*,2*H*-perfluorooctyl)silane was purchased from Sigma-Aldrich (St. Louis, MO). Infliximab was provided by Waters Corporation (Milford, MA), and mAb-A and mAb-B were provided by Pfizer Inc. (St. Louis, MO).

Sample Preparation. Monoclonal antibody samples were stored in their respective formulation buffers at −20 °C until analysis. Samples were thawed at room temperature and diluted to 1.0 mg/mL with an aqueous solution of 10% 2-propanol/0.2% acetic acid (pH 3.17). For Infliximab and mAb-B, no additional sample preparation was necessary. The formulation buffer of mAb-A contained a significantly higher level of salt than the other mAb samples, so the diluted sample was buffer exchanged with BGE using an Amicon Ultra Ultracel 50 kDa centrifugal filter (Millipore, Billerica, MA) prior to analysis. The final sample volume was 100 μL for all three mAbs.

Fabrication and Preparation of Microfluidic Devices. The design for the CE-ESI devices has been described previously.[38] As illustrated in Figure 1, the device incorporated an injection cross for sample handling, a 23 cm long separation channel, an electroosmotic pump for sustaining ESI, and an integrated ESI emitter. The turns in the separation channel were asymmetrically tapered to minimize band broadening contributions from varying path lengths around the turn.[39−43]

Standard photolithography and wet chemical etching techniques were used to fabricate the CE-ESI devices in house from 0.5 mm thick B270 glass wafers (PerkinElmer, Waltham, MA). All straight channels were etched to a depth and full width of 10 and 70 μm, respectively. The integrated ESI emitter was formed by dicing the corner of the device to 90° using a precision dicer from Dicing Technology Incorporated (Longwood, FL). The edges of the corner containing the ESI emitter were polished to remove dicing artifacts using 3 μm cerium oxide abrasive lapping paper and a lapping wheel (Ultra Tec, Santa Ana, CA). Buffer reservoirs were formed by attaching 8 mm diameter glass cylinders to the devices with chemically resistant epoxy (Loctite E-120HP, Henkel Corporation, Germany). The fluid capacity of the reservoirs is approximately 200 μL. Photographs of completed devices can be found in Figure S1 of the Supporting Information.

CE-ESI devices were coated with APDIPES via chemical vapor deposition.[38] The injection cross and separation channels were then covalently coated with NHS-PEG$_{450}$ through liquid phase PEGylation. A 10 mg/mL solution of NHS-PEG in 100

DOI: 10.1021/ac503964j
Anal. Chem. 2015, 87, 2264−2272

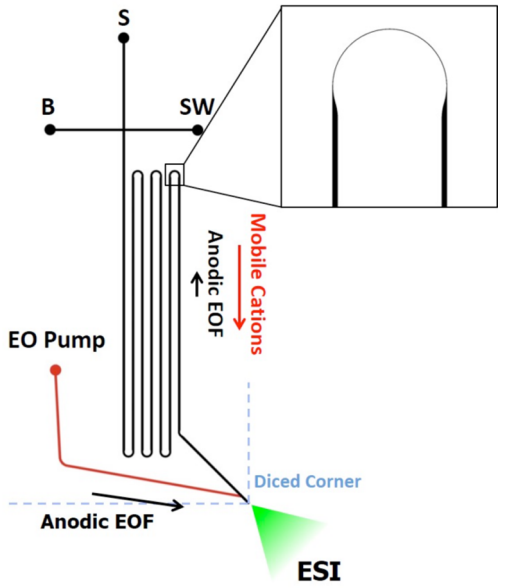


Figure 1. Schematic for CE-ESI devices with a 23 cm separation channel with an enlarged image of the asymmetric turn tapering. Red channels indicate an APS coating while black channels indicate an APS-PEG_{450} coating. S: sample reservoir; B: background electrolyte reservoir; SW: sample waste reservoir; EO: electroosmotic pump reservoir.

mM phosphate buffer (pH 7.5) was put in the sample (S), buffer (B), and sample waste (SW) reservoirs. Flow was maintained through the channels by the application of suction to the ESI emitter and 50 psi of head pressure to the S, SW, and B reservoirs. To create the electroosmotic pump, the EO pump channel was not PEGylated. The difference between the strong anodic EOF of the EO pump channel and the weak EOF of the PEGylated separation channel results in pressure-driven flow out of the ESI emitter when voltage is applied to the device as described below. With the low EOF surface coating in the separation channel, the integrated electroosmotic pump is vital to the successful formation of analyte ions; the pumping channel provides continuous fluid flow that is necessary for maintaining stable and sensitive ESI. Once the PEGylation process was complete, excess PEG reagent was rinsed from the channels with DI water by thoroughly rinsing all solvent reservoirs and then applying suction to the ESI emitter for 20 min. Device channels were then filled with background electrolyte by applying suction at the ESI emitter. After the coating procedures were completed, 5 μL of trichloro-(1*H*,1*H*,2*H*,2*H*-perfluorooctyl)-silane was applied to the ESI emitter to increase the hydrophobicity of the external surface and facilitate ESI. Excess reagent was removed with suction, and the surface was cured at room temperature for approximately 10 min.

CE-ESI-MS Device Operation and Data Analysis. CE-ESI devices were operated by applying voltage to the solvent reservoirs via platinum wire electrodes. The electrodes were powered by an in-house built power supply containing five UltraVolt modules (Ronkonkoma, NY): Three 0 to +20 kV modules (P/N 20A24-P15) to power reservoirs S, B, and SW (Figure 1) and two 0 to +10 kV modules (P/N 10A12-P4) to power the EO reservoir and the ESI shield electrode. The voltage output of the power supply was controlled via a custom LabVIEW (National Instruments, Austin, TX) program. An aqueous solution of 10% 2-propanol/0.2% acetic acid (pH 3.17) was used for all analyses. As denoted by the arrows in Figure 1, devices were operated such that highly mobile cations migrate against the low anodic EOF in the PEGylated channels. These cations can then be gated or manipulated for injection and separation at the injection cross. The typical voltage states used for operating the CE-ESI devices is given in Table 1.

Table 1. Representative Voltage Scheme for Sample Handling on the CE-ESI Device

	applied voltage (kV)	
	gate	inject
S	18	18
B	18	17
SW	16	17
EO	2	2
shield	0.5	0.5

Injection of the sample was performed by switching the voltage profile from the gated state to the injection state for 200 ms and back again. This resulted in the injection of ~175 pg of antibody. Minor differences in the amount injected are due to differences in the mobility of the antibodies and differences in the field strength used during analysis. Field strengths for each separation are provided in the respective figure captions. For this work, the full 100 μL of mAb sample was pipetted into the sample reservoir. However, it should be noted that only a small fraction of this is consumed during analysis and a significantly smaller sample volume could be used.

Devices were positioned in front of the inlet of the mass spectrometer using a custom built stage (Figures S3 and S4 of the Supporting Information). A shield electrode fabricated from single-sided copper clad circuit board (M.G. Chemical, Burlington, Ontario, Canada) was used to isolate the ESI emitter from the electric field generated by the high voltages powering the CE-ESI device. Throughout the analysis, +500 V was applied to the shield electrode. MS analysis was performed using a Waters LCT-Premier time-of-flight mass spectrometer (Waters Corporation, Milford, MA) operated in V-mode with the source at 150 °C. Data were acquired over a mass range of 2000−6500 m/z with a 0.2 s scan time. Data acquisition was accomplished through MassLynx (Waters Corporation) software, which was triggered through the LabVIEW program used to control the power supply output.

Deconvolution of the mass spectra was performed on the basis of maximum entropy analysis using the MaxEnt1 deconvolution algorithm in the MassLynx software. Resolution was set at 1.00 Da with minimum intensity ratios at 50%, and the software was set to perform 15 iterations to reduce the occurrence of deconvolution artifacts in the resulting spectrum.[6] The mass range and uniform Gaussian width at half height were adjusted to best match the specific set of data.[6,44] As described previously for deconvolution of intact mAbs spectra, the 5−6 most abundant charge state peaks were used to provide high signal-to-noise data for processing and reduce the potential side effects of adducts on high m/z ions.[45]

RESULTS AND DISCUSSION

Characterization of Infliximab. Infliximab is an IgG1 type antibody known to have nearly equal abundances of C-terminal lysine variants, giving a characteristic 3-peak separation profile when separated by charge.[46] With this knowledge, we can

DOI: 10.1021/ac503964j
Anal. Chem. 2015, 87, 2264−2272

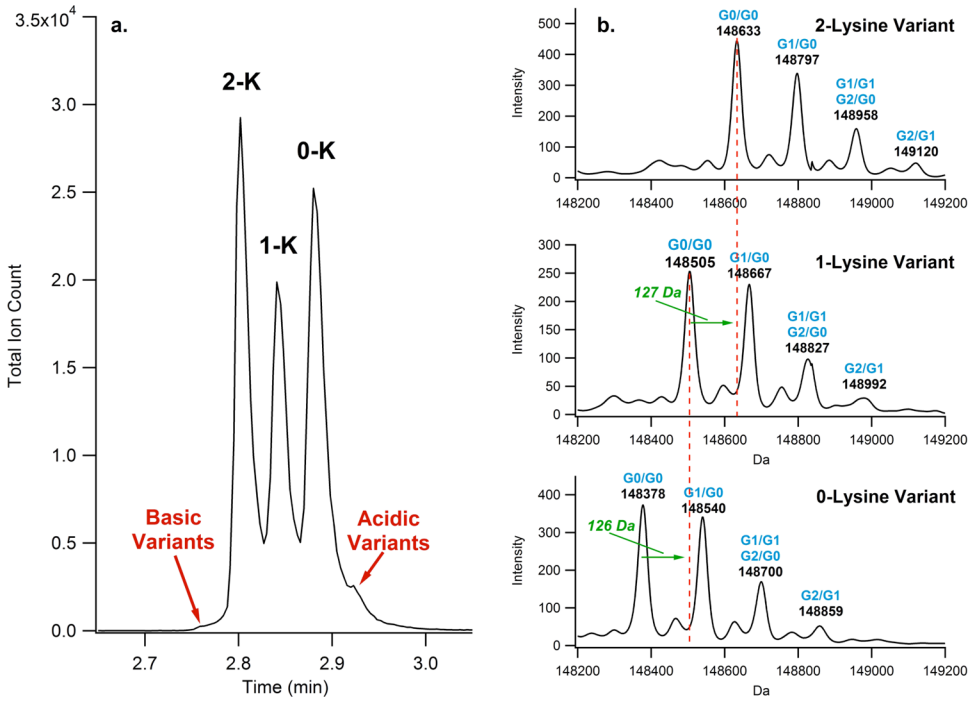


Figure 2. (a) Separation of intact Infliximab charge variants using a 23 cm APS-PEG$_{450}$ coated device at approximately 600 V/cm. Identified lysine variant bands are labeled as 2-K, 1-K, and 0-K. (b) Deconvoluted mass spectra for each lysine variant. Glycosylation structures are labeled above the mass of each peak.

expect to see a change in mobility due to the removal of a +1 charge associated with C-terminal lysine truncation and a 128 Da difference in mass between variants.[1] These characteristics make Infliximab a particularly useful analyte for the development and evaluation of an intact mAb analysis method. Figure 2a shows a microfluidic CE separation of Infliximab with ESI-MS detection. The separation profile is similar to CE separations of Infliximab reported in the literature using TETA and EACA BGE additives with optical detection.[32,33] However, with this analysis platform, these additives were unnecessary to achieve a comparable separation, and for the first time, intact mAb charge variants have been separated and identified by MS analysis using a single experiment. There are three nearly baseline resolved peaks along with smaller peaks to the left and right, indicating the presence of minor basic and acidic variants, respectively. The three largest peaks are on average 1.2 s duration at half height (~2 s duration at the base.) Mass spectra were generated by summing an approximately 2 s window of MS data points from the center of each peak in the electropherogram.

Deconvolution of each charge variant mass spectrum generated multiple masses, corresponding to the expected presence of neutral glycosylation variants. To facilitate discussion of the charge variants, the most abundant mass variant was used to describe the mass of the charge variant band. The less intense mass peaks present between the labeled mass peaks in the deconvoluted spectrum are believed to be deconvolution artifacts. Thus, as seen in Figure 2b, the masses ascribed to the three most abundant charge variant bands are 148 633, 148 506, and 148 380 Da. Representative raw data used to generate the deconvoluted spectra are given in Figure S4 of the Supporting Information. The difference in mass between these bands is similar to the expected mass shift associated with the addition of a lysine residue. On the basis of the MW information, the earliest band corresponds to the 2-lysine variant (2-K), the middle band corresponds to the 1-lysine variant (1-K), and the last band corresponds to the 0-lysine variant (0-K). This assignment is also supported by the change in apparent mobility (μ_{app}) of the variants. On the basis of three replicate electropherograms, the three bands correspond to μ_{app} values and relative standard deviations of 2.28×10^{-4} (±0.83%), 2.25×10^{-4} (±0.82%), and 2.22×10^{-4} (±0.83%) cm^2/(V s). The addition of each lysine residue increased the electrophoretic mobility by the same amount (0.03×10^{-4} cm^2/(V s)), implying that the variation between the charge variants is of the same nature.

In addition to the major lysine variants, there are also minor basic and acidic variants visible to the left and right of the three major peaks. These minor peaks deconvolute to MWs of 148 642 and 148 378 Da for the basic and acidic regions, respectively. Relating these minor variants to their nearest lysine variant peak equates to a 9 Da increase for the basic variant and a 2 Da decrease for the acidic variant. Although further work is required to identify these modifications, it is plausible that the mass shifts are a result of several cumulative modifications. For instance, two deamidations would cause a decrease in MW of 2 Da and also reduce the net charge of the mAb causing a μ_{app} decrease.[1] This is in agreement with the characteristics of the minor acidic variant and is a potential explanation for its modification. The low signal-to-noise ratio of the mass spectra associated with these low-abundance variants introduces error into the deconvolution process, and a more sensitive mass spectrometer with greater resolving power would improve the identification of these species.

An expected modification of antibodies that can significantly impact their immunogenic properties is glycosylation. IgGs have a conserved N-linked glycosylation site at an asparagine residue in the Fc domain of the heavy chain. The branched glycan structures enzymatically added at this site are primarily composed of N-acetylglucosamine, fucose, and mannose

DOI: 10.1021/ac503964j
Anal. Chem. 2015, 87, 2264−2272

residues but can differ in the number of terminal galactose residues. The addition of galactose moieties to the glycan structure is associated with a mass increase of 162 Da/moiety but does not induce a change in net charge.[1,5,47] While changes in mass have the potential to affect mobility, the mass of a galactose moiety accounts for only ~0.1% of the total mass of the antibody. To induce a μ_{app} shift on par to that associated with a change in net charge, the mass increase would have to be much greater or induce a significant change in conformation. Although there is not a mobility shift between mAb glycoforms, glycosylation patterns are visible in the mass spectra of the major charge variants of Infliximab. Glycoforms are labeled in Figure 2b above the associated mass peak. The addition of 0 to 2 galactose moieties per glycan structure is visible, and the various glycoforms are present in similar abundances for each lysine variant. While not observed here, it is worth noting that CE has the potential to resolve glycoforms with acidic glycans, due to a reduction in net charge from the addition of negatively charged sialic acid groups.[1]

The advantage of a separation prior to MS analysis is obvious when comparing the mass spectrum of Infliximab generated by direct infusion-MS to the mass spectra of the individual variant peaks produced by CE-ESI-MS. The infusion mass spectrum for the +31 charge state is given in Figure 3, and the

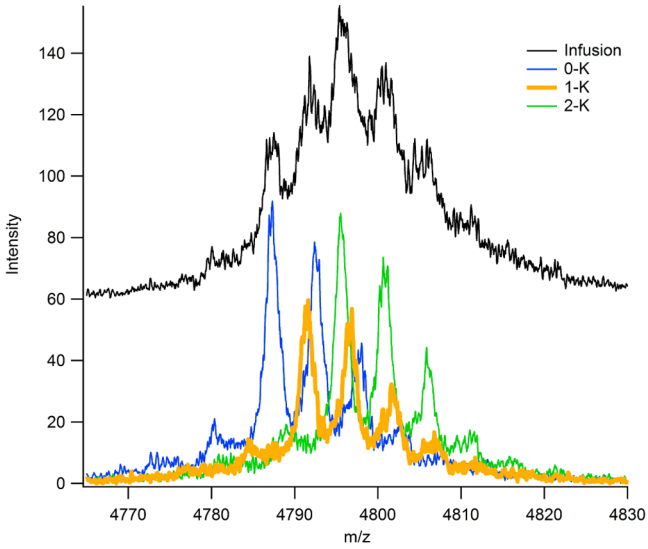


Figure 3. Direct infusion of Infliximab compared to overlaid spectra of the 0K−2K variants generated from the separation in Figure 2a. The 1-K variant spectrum is in bold to show detail.

comparable charge states of the three lysine variants are overlaid beneath the infusion spectrum. The overlaid lysine variant spectra depict how the mAb species overlap and combine to obscure individual mass signals if they are not separated prior to MS analysis. As described in Figure 2b, at least 4 mAb glycoforms can be identified per lysine variant, resulting in at least 12 mAb species identified. However, there are only six distinct features in the infusion spectrum due to spectral overlap of the lysine variants. The result of this is a more convoluted mass spectrum with wider m/z peaks (fwhm ~5 m/z) as opposed to the separated variant spectra (fwhm ~2 m/z). The deconvolution algorithm is incapable of generating MWs for the different glycoforms of each lysine variant from the infusion mass spectrum. Only seven MWs are generated that are not easily interpreted because they are a combination of multiple mAb mass signals (data not shown). Additionally, the minor acidic and basic variants are completely obscured due to their low abundance and small mass shifts. Having a CE separation in line with MS detection results in simpler mass spectra and, in turn, the identification of more mAb species. While an instrument with state of the art resolving power will resolve more mass species during an infusion experiment than the instrument used for this work, the simplification of the mAb population achieved through separation reduces the requirements for MS resolving power. The microfluidic CE-ESI-MS approach, in turn, renders this type of mAb analysis available to laboratories with modest MS resolving power, i.e., a few thousand.

Characterization of mAb-A and mAb-B. To test the general applicability of this CE-ESI-MS method for the characterization of biotherapeutics, two additional mAbs were analyzed. The mAb-A molecule is an IgG2 type antibody, and a separation of this mAb is given in Figure 4a. There are four distinct product related bands present in the electropherogram. The MWs generated from deconvoluting the mass spectra associated with each band are 146 407, 146 277, 146 146, and 146 169 Da for bands 1−4, respectively. The mass differences between the first three bands are approximately 130 Da, corresponding to a shift associated with a C-terminal lysine residue. The 2−3 Da difference between the expected and observed mass shifts is likely due to both the signal intensity of the smaller charge variant peaks and error associated with the deconvolution process. To support the identification of these as lysine variants, the μ_{app} of each species was calculated. Bands 1−3 have μ_{app} values of 2.09×10^{-4} (±0.023%), 2.06×10^{-4} (±0.057%), and 2.03×10^{-4} (±0.043%) $cm^2/(V\ s)$, respectively. The trend of decreasing μ_{app} with decreasing MW that was seen with Infliximab is also followed with mAb-A. Additionally, the difference in mobility of the mAb-A charge variants under these conditions is 0.03×10^{-4} $cm^2/(V\ s)$, which is identical to the μ_{app} shift between the lysine variants of Infliximab. Bands 1−3 can therefore be characterized as 2-K, 1-K, and 0-K, respectively. This strategy of using electrophoretic mobility shifts to support identification could potentially be applied as a metric for analyzing other mAb modifications. Although both mAb-A and Infliximab have C-terminal lysine variants, the relative variant abundances are very different. The mAb-A material is perhaps more indicative of a typical biotherapeutic mAb in that the partial C-terminal lysine truncation variants account for a relatively small percentage of the total mAb population. The mAb-A and Infliximab data were analyzed using the Igor Pro Multipeak Fitting 2 analysis package, and the results of the fit were used to approximate the relative abundance of C-terminal lysine variants for each molecule. On the basis of peak areas from the total ion electropherogram for the C-terminal lysine variants, it was determined that mAb-A is composed of 2% 2-K variant, 6% 1-K variant, and 92% 0-K variant, while Infliximab is approximately 34% 2-K variant, 28% 1-K variant, and 38% 0-K variant. Glycosylation patterns are also visible in the mass spectra associated with the identified lysine variants for mAb-A. Glycoform labels are designated above the peak masses in Figure 4b. The addition of up to four galactose residues is visible in the mass spectrum for the major 0-K charge variant peak. The most acidic variant, peak 4, differs in mass from the 0-K variant (peak 3) by 23 Da. The nature of this modification is not immediately obvious and, therefore, could be a combination of variations to the structure that also results in

DOI: 10.1021/ac503964j
Anal. Chem. 2015, 87, 2264−2272

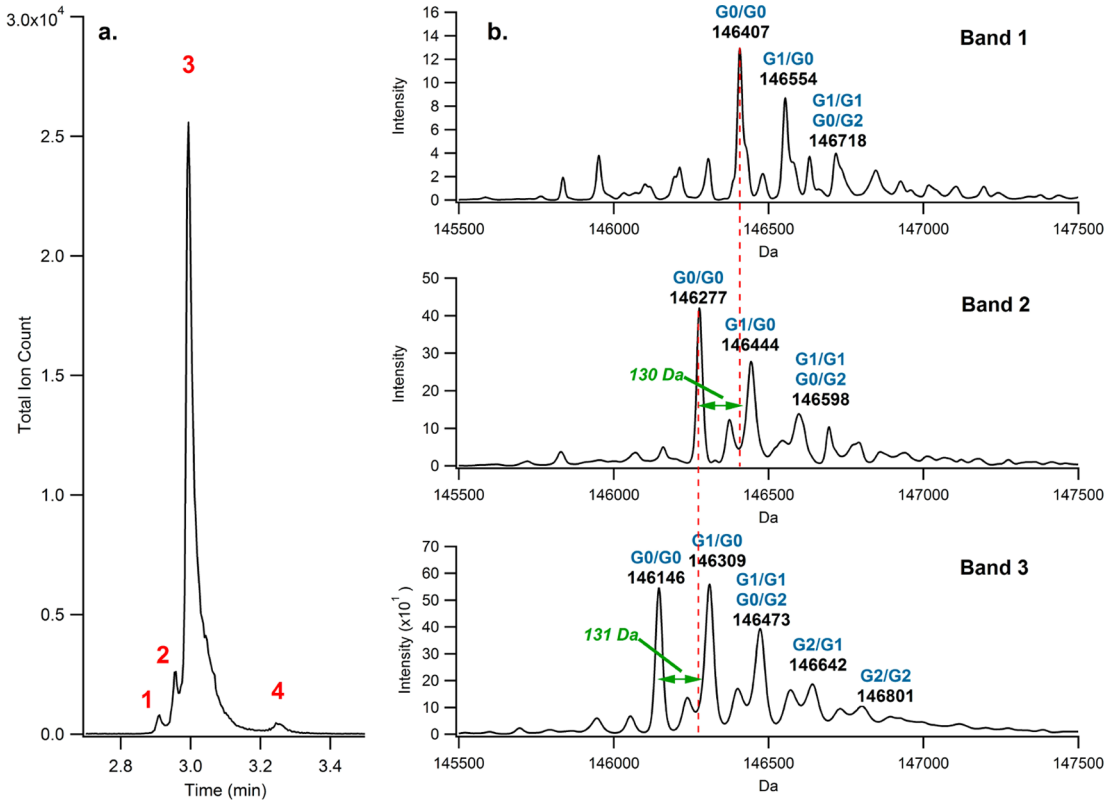


Figure 4. (a) Separation of 1 mg/mL mAb-A using a 23 cm APS-PEG$_{450}$ coated device at approximately 600 V/cm. (b) Deconvoluted mass spectra for each major variant band. Glycosylation structures are labeled above each mass spectral peak.

a net charge reduction as supported by the observable shift in μ_{app}.

The mAb-B molecule is an IgG1 with a bioactive peptide conjugated to the antibody scaffold in the Fab domain of the heavy chain through conventional lysine based chemistry.[48] It is expected that most of the molecules within the total population of mAb-B have a conjugate on each heavy chain; however, there may be some singly- or unconjugated species present. The analysis of the mAb-B conjugate using conditions optimized for signal and separation resolution is given in Figure 5a. On the basis of the electropherogram alone, it could be reasoned that these bands correspond to different levels of conjugation: the smaller band being mAb species with a single conjugation and the larger, broader band being the more abundant doubly conjugated mAb species. However, the mass spectra associated with bands 1 and 2 deconvolute to MWs of 151 914 and 151 964 Da, respectively. The mass shift of only 51 Da is not enough to be attributed to conjugation differences. Potentially, it is due to multiple modifications that together result in a change in net charge. A second charge envelope is present in the raw mass spectrum of band 2 (Figure 5b) and deconvolutes to the lower MW of 150 836 Da (Figure 5c). This mass difference (1128 Da) is large enough to correspond to a difference in conjugation within the mAb population.

The conjugation is a more significant mass difference than the addition of a galactose moiety, accounting for ~0.7% of the MW, so a μ_{app} shift may be observable. As seen in Figure 6, extracted ion electropherograms for the most abundant charge state from each envelope (3706−3720 m/z for the doubly conjugated species and 3863−3882 m/z for the singly conjugated species) reveal that the species differ in migration time by 0.010 min (0.60 s), which equates to a μ_{app} difference of 0.0073×10^{-4} cm^2/(V s). The calculated resolution between the two conjugation variants is 0.2. Conversely, the C-terminal lysine residues on Infliximab with a 0.03×10^{-4} cm^2/(V s) difference in μ_{app} resulted in an average resolution of 0.80 between variants. The partial resolution between the conjugated mAb species is obscured in the electropherogram by the nearly 5-fold difference in intensity between the peaks. However, the mass spectral information can be used to determine that peak 2 is not solely due to a single mAb species but is a combination of two mAb variants.

Analysis of the mAb-B antibody conjugate highlights the usefulness of the CE-ESI-MS approach. The mass spectral information prevented the first band from being mistakenly identified as a conjugation variant. Although the two conjugation species were not fully resolved, it is likely that differences in antibody conjugation could be resolved if the conjugation was charged, of greater mass, or both. However, information about the extent of conjugation can still be obtained from the mass spectrum of peak 2 even though the two species are not fully resolved in the CE domain.

CONCLUSION

Here, we have demonstrated a microfluidic CE-ESI-MS method for the separation of intact mAb charge variants. To the best of our knowledge, this is the first demonstration of intact mAb charge variant separations with online ESI-MS detection. The surface chemistry utilized in the device channels suppressed the EOF and prevented analyte adsorption, eliminating the need for complex BGE additives. The microfluidic ESI interface proved vital to the successful ionization and resulting MS analysis by maintaining fluid flow to generate stable ESI. The use of an ESI compatible BGE and the efficient microfluidic ESI

DOI: 10.1021/ac503964j
Anal. Chem. 2015, 87, 2264−2272

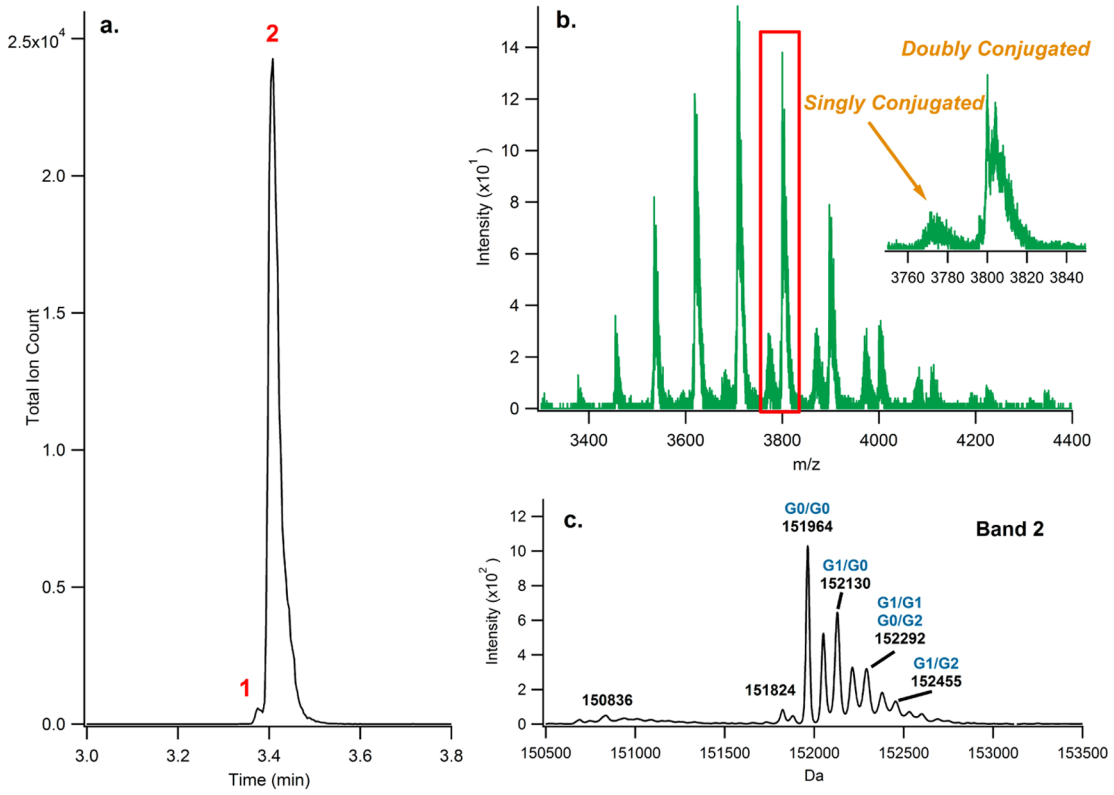


Figure 5. (a) Separation of 0.5 mg/mL mAb-B using a 23 cm APS-PEG$_{450}$ coated device at approximately 470 V/cm. (b) Raw mass spectrum associated with band 2. The low intensity charge state peaks corresponding to the unconjugated species are visible between the higher intensity charge state peaks of the conjugated species. (c) Deconvolution of the mass spectrum in (b). Glycoforms are labeled above the mass of the peak. Additional unlabeled mass peaks are believed to be deconvolution artifacts that result from the limited resolution obtained in the mass domain for this molecule.

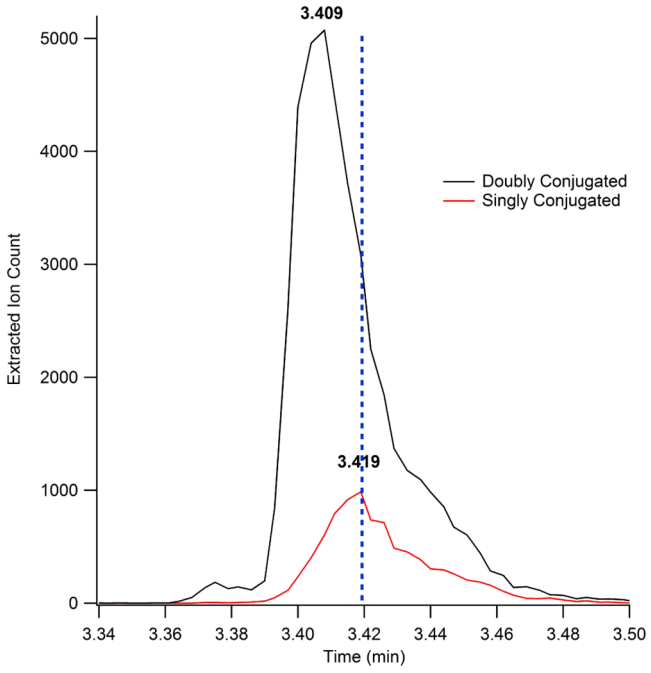


Figure 6. Extracted ion electropherograms for the most abundant charge state of the doubly and singly conjugated mAb species of mAb-B.

interface enabled MS analysis of the intact mAb charge variants. Molecular weights were determined for five charge variants detected in the separation of Infliximab through deconvolution of the mass spectra. Three C-terminal lysine variants were identified by characteristic 128 Da mass shifts, and this identification was supported by the increase in cationic μ_{app} with the addition of a lysine residue to the mAb species. Thus, this analysis platform yields two criteria to aid in the identification of mAb charge variants: mass and electrophoretic mobility. The advantage of adding a separation step prior to MS analysis of intact monoclonal antibodies is evident when comparing direct infusion mass spectra to spectra generated from separation data. Individually analyzing mAb variants results in simplified MS data and increases the number of mAb species that can be identified from the analysis. The separation of Infliximab charge variants allowed the glycoforms of the variants to be characterized; the addition of 0 to 4 galactose residues to the glycan structure was identified in the deconvoluted spectra of the major variant bands.

Two additional mAbs were analyzed to demonstrate the general applicability of our approach. The antibody, mAb-A, proved to bear similar modifications to Infliximab. Three C-terminal lysine variants were identified by mass and confirmed by the same electrophoretic mobility shift observed for the Infliximab sample. While the lysine variants of Infliximab were of roughly equal abundance, the 1-K and 2-K variants of mAb-A were estimated to account for only 6% and 2% of the total population of mAb-A. For the antibody drug conjugate, mAb-B, it was determined that the two resolved bands in the electropherogram were not due to conjugation differences expected to be seen in the mAb population. Rather, the mAb species bearing one conjugation was partially resolved but

DOI: 10.1021/ac503964j
Anal. Chem. 2015, 87, 2264−2272

obscured by the high signal intensity of the doubly conjugated species. This was evident in the mass spectrum associated with the major electrophoretic band produced by this sample. The singly conjugated mAb species would otherwise be invisible if optical detection was used.

These results demonstrate that the microfluidic CE-ESI device strategy described here is a rapid, generic strategy for the separation of intact mAb charge variants and allows direct coupling to MS analysis. This approach generates multiple pieces of information in a single analysis step. The mass of intact mAb variants, an assessment of charge heterogeneity, and glycoform information are all obtained with little to no sample preparation and total analysis times of less than 4 min. The electrophoretic separation of mAb variants prior to MS analysis reduces the performance requirements of the MS instrument needed to characterize the mAb. MS instrumentation with greater mass accuracy and sensitivity would indeed facilitate the identification of mAb variants while using the separation device but is not a requirement for successful analysis. The CE separation could also be improved by utilizing higher voltages to increase the resolution between mAb charge variants and further reduce analysis times.

■ ASSOCIATED CONTENT

Supporting Information

Additional information about the laboratory setup for microfluidic CE-ESI coupled to MS instrumentation. Unprocessed mass spectra for each of the mAbs analyzed. This material is available free of charge via the Internet at http://pubs.acs.org.

■ AUTHOR INFORMATION

Corresponding Author

*E-mail: jmramsey@unc.edu. Fax: 919-962-2388.

Notes

The authors declare no competing financial interest.

■ ACKNOWLEDGMENTS

We would like to thank the National Institutes of Health (Grant 5R01GM066018-11) and the University of North Carolina at Chapel Hill Center for Biomedical Microdevices for support of this work; Waters Corporation for providing Infliximab; and Pfizer Inc. for providing mAb-A and mAb-B. We also thank Dr. Jason A. Starkey, of Pfizer Inc., for his insightful contributions to this manuscript.

■ REFERENCES

(1) Liu, H.; Gaza-bulseco, G.; Faldu, D.; Chumsae, C.; Sun, J. *J. Pharm. Sci.* **2008**, *97*, 2426−2447.
(2) Fekete, S.; Gassner, A.-L.; Rudaz, S.; Schappler, J.; Guillarme, D. *TrAC, Trends Anal. Chem.* **2013**, *42*, 74−83.
(3) Macht, M. *TrAC, Trends Anal. Chem.* **2013**, *48*, 62−71.
(4) Zhang, H.; Cui, W.; Gross, M. L. *FEBS Lett.* **2014**, *588*, 308−317.
(5) Arnold, J. N.; Wormald, M. R.; Sim, R. B.; Rudd, P. M.; Dwek, R. A. *Annu. Rev. Immunol.* **2007**, *25*, 21−50.
(6) Zhang, Z.; Pan, H.; Chen, X. *Mass Spectrom. Rev.* **2009**, *28*, 147−176.
(7) Chelius, D.; Jing, K.; Lueras, A.; Rehder, D. S.; Dillon, T. M.; Vizel, A.; Rajan, R. S.; Li, T.; Treuheit, M. J.; Bondarenko, P. V. *Anal. Chem.* **2006**, *78*, 2370−2376.
(8) Jones, L. M.; Zhang, H.; Cui, W.; Kumar, S.; Sperry, J. B.; Carroll, J. A.; Gross, M. L. *J. Am. Soc. Mass Spectrom.* **2013**, *24*, 835−845.
(9) Beck, A.; Diemer, H.; Ayoub, D.; Debaene, F.; Wagner-Rousset, E.; Carapito, C.; Van Dorsselaer, A.; Sanglier-Cianférani, S. *TrAC, Trends Anal. Chem.* **2013**, *48*, 81−95.
(10) Valeja, S. G.; Kaiser, N. K.; Xian, F.; Hendrickson, C. L.; Rouse, J. C.; Marshall, A. G. *Anal. Chem.* **2011**, 8391−8395.
(11) Rea, J. C.; Moreno, G. T.; Lou, Y.; Farnan, D. *J. Pharm. Biomed. Anal.* **2011**, *54*, 317−323.
(12) Farnan, D.; Moreno, G. T. *Anal. Chem.* **2009**, *81*, 8846−8857.
(13) Rozhkova, A. *J. Chromatogr., A* **2009**, *1216*, 5989−5994.
(14) Talebi, M.; Nordborg, A.; Gaspar, A.; Lacher, N. A.; Wang, Q.; He, X. Z.; Haddad, P. R.; Hilder, E. F. *J. Chromatogr., A* **2013**, *1317*, 148−154.
(15) Mokaddem, M.; Gareil, P.; Varenne, A. *Electrophoresis* **2009**, *30*, 4040−4048.
(16) Alvarez, M.; Tremintin, G.; Wang, J.; Eng, M.; Kao, Y.-H.; Jeong, J.; Ling, V. T.; Borisov, O. V. *Anal. Biochem.* **2011**, *419*, 17−25.
(17) Lucy, C. A.; MacDonald, A. M.; Gulcev, M. D. *J. Chromatogr., A* **2008**, *1184*, 81−105.
(18) Stutz, H. *Electrophoresis* **2009**, *30*, 2032−2061.
(19) Huhn, C.; Ramautar, R.; Wuhrer, M.; Somsen, G. W. *Anal. Bioanal. Chem.* **2010**, *396*, 297−314.
(20) Haselberg, R.; de Jong, G. J.; Somsen, G. W. *Electrophoresis* **2013**, *34*, 99−112.
(21) Gahoual, R.; Busnel, J.; Beck, A.; Leize-wagner, E. *Anal. Chem.* **2014**, *86*, 9074−9081.
(22) Gahoual, R.; Burr, A.; Busnel, J.-M.; Kuhn, L.; Hammann, P.; Beck, A.; François, Y.-N.; Leize-Wagner, E. *MAbs* **2013**, *5*, 1−12.
(23) Whitmore, C. D.; Gennaro, L. A. *Electrophoresis* **2012**, *33*, 1550−1556.
(24) Sun, L.; Knierman, M. D.; Zhu, G.; Dovichi, N. J. *Anal. Chem.* **2013**, *85*, 5989−5995.
(25) Haselberg, R.; de Jong, G. J.; Somsen, G. W. *J. Sep. Sci.* **2009**, *32*, 2408−2415.
(26) Haselberg, R.; de Jong, G. J.; Somsen, G. W. *Anal. Biochem.* **2013**, *85*, 2289−2296.
(27) Ramautar, R.; de Jong, G. J.; Somsen, G. W. *Electrophoresis* **2012**, *33*, 243−250.
(28) Haselberg, R.; Brinks, V.; Hawe, A.; de Jong, G. J.; Somsen, G. W. *Anal. Bioanal. Chem.* **2011**, *400*, 295−303.
(29) He, Y.; Isele, C.; Hou, W.; Ruesch, M. *J. Sep. Sci.* **2011**, *34*, 548−555.
(30) Shi, Y.; Li, Z.; Qiao, Y.; Lin, J. *J. Chromatogr., B* **2012**, *906*, 63−68.
(31) He, Y.; Lacher, N. A.; Hou, W.; Wang, Q.; Isele, C.; Starkey, J.; Ruesch, M. *Anal. Chem.* **2010**, *82*, 3222−3230.
(32) Gassner, A.-L.; Rudaz, S.; Schappler, J. *Electrophoresis* **2013**, *34*, 2718−2724.
(33) Espinosa-de la Garza, C. E.; Perdomo-Abúndez, F. C.; Padilla-Calderón, J.; Uribe-Wiechers, J. M.; Pérez, N. O.; Flores-Ortiz, L. F.; Medina-Rivero, E. *Electrophoresis* **2013**, *34*, 1133−1140.
(34) Chambers, A. G.; Mellors, J. S.; Henley, W. H.; Ramsey, J. M. *Anal. Chem.* **2011**, *83*, 842−849.
(35) Mellors, J. S.; Black, W. A.; Chambers, A. G.; Starkey, J. A.; Lacher, N. A.; Ramsey, J. M. *Anal. Chem.* **2013**, *85*, 4100−4106.
(36) Mellors, J. S.; Gorbounov, V.; Ramsey, R. S.; Ramsey, J. M. *Anal. Chem.* **2008**, *80*, 6881−6887.
(37) Mellors, J. S.; Jorabchi, K.; Smith, L. M.; Ramsey, J. M. *Anal. Chem.* **2010**, *82*, 967−973.
(38) Batz, N. G.; Mellors, J. S.; Alarie, J. P.; Ramsey, J. M. *Anal. Chem.* **2014**, *86*, 3493−3500.
(39) Culbertson, C. T.; Jacobson, S. C.; Ramsey, J. M. *Anal. Chem.* **2000**, *72*, 5814−5819.
(40) Culbertson, C. T.; Jacobson, S. C.; Ramsey, J. M. *Anal. Chem.* **1998**, *70*, 3781−3789.
(41) Jacobson, S. C.; Hergenroder, R.; Koutny, L. B.; Ramsey, J. M. *Anal. Chem.* **1994**, *66*, 1114−1118.
(42) Jacobson, S. C.; McKnight, T. E.; Ramsey, J. M. *Anal. Chem.* **1999**, *71*, 4455−4459.
(43) Jacobson, S. C.; Hergenroder, R.; Koutny, L. B.; Warmack, R. J.; Ramsey, J. M. *Anal. Chem.* **1994**, *66*, 1107−1113.
(44) Ferrige, A. G.; Seddon, M. J.; Green, B. N.; Jarvix, S. A.; Skilling, J. *Rapid Commun. Mass Spectrom.* **1992**, *6*, 707−711.

DOI: 10.1021/ac503964j
Anal. Chem. 2015, 87, 2264−2272

(45) Berger, S. J.; Chen, W. *Efficiently Comparing Batches of an Intact Monoclonal Antibody Using the Biopharmalynx Software Package*, Waters Corporation Application Note, Number APNT10094155; Waters Corporation: Milford, MA, 2008.
(46) Shion, H.; Chen, W. *Structural Comparison of Infliximab and a Biosimilar via Subunit Analysis Using the Waters Biopharmaceutical Platform with UNIFI*, Waters Corporation Application Note, Number APNT134769667; Waters Corporation: Milford, MA, 2013.
(47) Raju, T. S.; Scallon, B. J. *Biochem. Biophys. Res. Commun.* **2006**, *341*, 797−803.
(48) Doppalapudi, V. R.; Huang, J.; Liu, D.; Jin, P.; Liu, B.; Li, L.; Desharnais, J.; Hagen, C.; Levin, N. J.; Shields, M. J.; Parish, M.; Murphy, R. E.; Del Rosario, J.; Oates, B. D.; Lai, J.-Y.; Matin, M. J.; Ainekulu, Z.; Bhat, A.; Bradshaw, C. W.; Woodnutt, G.; Lerner, R. A.; Lappe, R. W. *Proc. Natl. Acad. Sci. U. S. A.* **2010**, *107*, 22611−22616.

DOI: 10.1021/ac503964j
Anal. Chem. 2015, 87, 2264−2272